Communications in Information and Systems
Volume 23, Number 2, 185–212, 2023

# Quantitative anatomy of characteristics and influencing factors of PM2.5 and O3 in Liaoning province of China*

Hongmei Yang,
Yanqi Liu,
Xiaoqiu Jiang, and Xinqi Gong

Northeast China is an important region in Asia, bordered by Siberia to the north and Bohai Sea and Yellow Sea to the south. Liaoning province is one of the most important industrial and agricultural bases in China. It is located in the south of Northeast China. Due to the unique characteristics of geography, climate and anthropogenic emissions, it is of great significance to explore the air pollution in Liaoning Province. In this paper, spatial association network feature analysis, spatial interpolation, standard deviation ellipse and exploratory spatial data analysis are used to analyze the temporal and spatial evolution characteristics and influencing factors of PM2.5 and O3 in Liaoning Province. The results demonstrate that PM2.5 concentration has a decreasing trend in all cities, while O3 concentration has no obvious decreasing trend. The high concentration of PM2.5 is mainly distributed in central and northern of Liaoning, while high concentration of O3 is in central-western and coastal cities. PM2.5 and O3 show opposite seasonal dynamic characteristic, which is mainly due to their seasonal anthropogenic emissions, meteorological factors conducive to pollutant generation and geographical conditions unfavorable to the diffusion of air pollutants. Moreover, PM2.5 and O3 have certain spatial correlation with economic factors, such as agriculture, industry, tertiary industry and population density. The results of this study enable a more comprehensive understanding of the temporal and spatial distribution characteristics and the relative influencing factors of PM2.5 and O3 in Liaoning Province. This provides a policy basis for regional joint prevention and control and collaborative air pollution control in Northeast China.

Keywords and phrases: PM2.5, O3, quantitative anatomy.

*Research supported in part by the National Natural Science Foundation of China (No. 31670725).

## 1. Introduction

China is the largest developing country in the world and has achieved remarkable economic growth in the past decades. However, this is also accompanied by serious air pollution. In particular, PM2.5 and O3 are the two most serious air pollutants [1]. PM2.5 refers to fine particulate matter with a diameter less than or equal to 2.5 $\mu g/m^3$, which profoundly affects the environment and public health in different ways by hanging in the air for a long time, including human health [2], climate [3], agriculture and other ecosystems [4] and visibility [5]. O3 is a photochemical pollutant, potentially harmful to human health [2]. In order to cope with the serious air pollution problems, China's State Council has implemented a series of emission control policies to improve air quality in the last decade, including the Action Plan of Air Pollution Prevention and Control (2013–2017) [6], and the Three-Year Action Plan to Win the Battle for a Blue Sky (2018–2020) [7]. Thanks to the measures, the concentration of PM2.5 in many parts of China reduced greatly during this period [8, 9, 10, 11]. However, it is worth noting that the concentration of O3 increased significantly in most regions simultaneously [12, 13, 14]. For example, the increase rates of O3 concentration in the North China Plain, Yangtze River Delta and Pearl River Delta are about 27%, 19% and 8%, respectively [15]. It can be seen from their chemical reaction mechanism that they all share common precursor, i.e., VOCs and NOx. And there may be a relationship between their pollution conditions [16]. PM2.5 and O3 dominate air quality by interacting with each other through photochemical reactions [17, 18]. PM2.5 and O3 are chemically coupled, and this coupling has profound implications for understanding the processes that control their levels [19]. Therefore, PM2.5 and O3 are considered to have a significant correlation. They may have collaborative effects and become more complex mixed pollutants, which may bring greater harm to national production and life [20, 21]. Effective reduction of the two pollutants also becomes more complex and difficult. In order to take correct reduction measures and effectively reduce and control these two new complex mixed pollutants, it is very important to deeply understand the spatial-temporal dynamic characteristics, collaborative change rules and possible influencing factors of these two new complex mixed pollutants.

Based on these studies, China is one of the world's worst polluters of PM2.5 and O3 [22, 23, 24]. PM2.5 and O3 have been studied on their variation, correlation and potential influencing factors at local, regional and national levels, aiming to provide guidance for collaborative control in many aspects [25, 26, 27, 28]. Nevertheless, the collaborative control of PM2.5 and

O3 still faces many obstacles, partly because their relationship is complex and difficult to quantify, and the reaction mechanisms have not been fully identified [29, 30]. Many studies concentrated on the characteristics and influence mechanism of PM2.5 and O3 in recent years. From the regional perspective, the areas with heavy PM2.5 pollution in winter were usually the same as those with heavy O3 pollution in summer. In some areas with obvious PM2.5 pollution alleviation, the deterioration of O3 pollution was severe. For instance, the Beijing-Tianjin-Hebei region and its surrounding areas [31], which may be caused by the sensitivity of O3-NOx-VOCs [32, 33]. From the temporal perspective, it was found that PM2.5 and O3 concentrations in many cities were related to seasons. They were positively correlated on the warm season. It was because the higher O3 concentration on the warm season would significantly promote the generation of secondary aerosols, which was conducive to PM2.5 generation. In cold season, it was the opposite; they showed as negatively correlated, mainly because atmospheric oxidation was weak, and the high concentration of PM2.5 in winter weakened solar radiation and inhibited atmospheric photochemical reaction, not conducive to the generation of O3 [34, 35, 36, 37, 38]. Meteorological factors played a crucial role in the interaction between PM2.5 and O3 [39, 40]. Dai et al. [41] found that the co-pollution time of PM2.5 and O3 was closely related to relative humidity, surface air temperature and wind speed in the Yangtze River Delta. In addition, numerous experimental studies on PM2.5 and O3 have been quantitatively conducted. To study the relationship between air pollution and other factors, including underway measurements, 3D numerical simulation and smog chamber, would require expensive large-scale experiments. Requirements on hardware, operators and time, and insufficient understanding of the complex physical and chemical reactions between PM2.5 and O3, which would inevitably lead to simulation errors [42, 43, 44]. Distributed lag nonlinear model (DLNM) showed good performance when it was used to analyze the effects of various influencing factors on PM2.5 and O3 [45, 46]. Collaborative control and effective management of PM2.5 and O3 pollution was the top concern of China's 14th Five-Year Plan (2020–2025) [47]. The multi-technology, multi-scale and multi-angle analysis results could provide a basis for the characteristics of air pollution in providing scientific support for the joint prevention and control of PM2.5 and O3 in the new stage.

Northeast China is an important region in Asia, bordered by Siberia to the north, Bohai Sea and Yellow Sea to the south. Most of the area is surrounded by three mountains, which are not conducive to the diffusion of air pollutants. Liaoning province lies in the south of northeast China. It is cold

here in winter, and heating is needed for half a year [48, 49]. Heating fuels include coal, biomass, natural gas and burning of agricultural straw, which release more air pollutants than other regions [50, 51, 52, 53]. Liaoning is also the heavy industrial base of China's steel, petroleum, petrochemical, shipbuilding, machine tools and other industries. Most of these heavy industries are traditional industries with high-energy consumption and high-pollution, which is another important cause of air pollution. Although China has implemented a series of air quality control measures, which have greatly improved PM2.5 concentration in northeast, O3 pollution still exists. Based on the unique geographical, climate, anthropogenic characteristics and heavy industrial structure, understanding the distribution characteristics and influencing factors of PM2.5 and O3 in the region have become one of the key problems of air pollution prevention and control in the northeast [54, 55]. Therefore, this paper analyzes the spatial-temporal evolution characteristics and spatial influencing factor of PM2.5 and O3 in Liaoning province, based on spatial association network feature analysis, spatial interpolation, standard deviation ellipse and exploratory spatial data analysis. This is an attempt to provide reference basis for regional joint prevention and control and collaborative air pollution control in Northeast China.

## 2. Materials and methods

### 2.1. Study area

Liaoning province is $118°53' \sim 125°46'E$, $38°43' \sim 43°26'N$. The terrain of the region is roughly sloped from north to south, from east and west to the middle. The east and the west of the region are mountains and hills, descending into the central plains, taking a horseshoe shape and sloped into Bohai Sea. Liaoning has a temperate monsoonal climate, the winter is cold and long, lasting 4–6 months, the minimum monthly mean temperature is $-12°C$ to $-19°C$, and lots of precipitation in summer. The studies have suggested that heating fuels has become one of the main sources of air pollution in the region, for instance, coal, biomass, natural gas and burning of agricultural straw. Burning of agricultural straw is used for rural heating in late autumn and early spring tillage, leading to a large number of air pollutants being directly released into the atmosphere [50, 51, 52, 53]. Liaoning is the most populous province in northeast China, which is an important base of commodity grain, heavy industry, animal husbandry and forestry in the region. Liaoning Province consists of 14 cities, which are Chaoyang, Fuxin, Shenyang, Tieling, Liaoyang, Anshan, Benxi, Fushun, Huludao, Jinzhou,

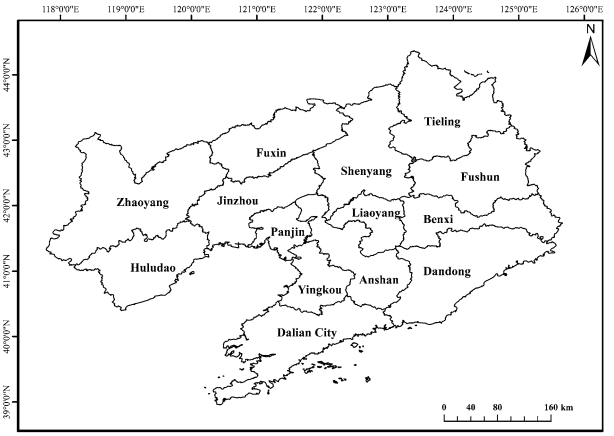


Figure 1: Geographical locations of 14 cities in Liaoning province.

Panjin, Yingkou, Dandong and Dalian. The locations of these 14 cities are showed in Fig. 1 and Table 1.

### 2.2. Data sources

Daily data of PM2.5 and O3 in 14 cities from January 1, 2016 to December 31, 2020 were downloaded from the China Air Quality Monitoring Platform. According to the environmental air quality standard (GB 3095-2012) modification list about the requirement in China, Table 2 was the concentration limits of PM2.5 and O3 at different levels. PM2.5 was evaluated by daily average, while O3 was evaluated by 8h. Economic statistics data in 2019 were from the Statistical Yearbook of Liaoning Province (http://tjj.ln.gov.cn/).

### 2.3. Method

Spatial-temporal dynamic analysis is an important method to accurately recognize, evaluate and comprehensively understand the spatial-temporal characteristics and interactions of pollutant distribution [56]. The spatial and temporal distribution characteristics and influencing factors of PM2.5 and O3 in Liaoning province were analyzed based on spatial association network feature analysis, spatial interpolation method, standard deviation ellipse method and exploratory spatial data analysis method.

Table 1: 14 cities in Liaoning province

| City number | City name | Latitude/degree | Longitude/degree |
|---|---|---|---|
| 1 | Chaoyang | 41.58 N | 120.42 E |
| 2 | Fuxin | 42.00 N | 121.65 E |
| 3 | Shenyang | 41.80 N | 123.38 E |
| 4 | Huludao | 40.71 N | 120.84 E |
| 5 | Jinzhou | 41.13 N | 121.15 E |
| 6 | Panjing | 41.12 N | 122.07 E |
| 7 | Anshan | 41.11 N | 122.99 E |
| 8 | Liaoyang | 41.27 N | 123.24 E |
| 9 | Benxi | 41.3 N | 123.73 E |
| 10 | Fushun | 41.97 N | 123.97 E |
| 11 | Tieling | 42.32 N | 123.85 E |
| 12 | Dandong | 40.13 N | 124.37 E |
| 13 | Dalian | 38.92 N | 121.62 E |
| 14 | Yingkou | 40.65 N | 122.18 E |

Table 2: The concentration limits at different levels for PM2.5, O3 and AQI. Unit: $\mu g/m^3$ for PM2.5 and O3

| AQI levels | AQI value | Air quality level | PM2.5 | O3 |
|---|---|---|---|---|
| *I* | 0–50 | good | 0–35 | 0–100 |
| *II* | 51–100 | moderate | 36–75 | 101–160 |
| *III* | 101–150 | lightly polluted | 76–115 | 161–215 |
| *IV* | 151–200 | moderately polluted | 116–150 | 216–265 |
| *V* | 201–300 | heavily polluted | 151–250 | 266–800 |
| *VI* | >300 | Severely polluted | >250 | >800 |

**2.3.1. The standard deviation ellipse method** The temporal dynamics process of PM2.5 and O3 in Liaoning Province was characterized by standard deviation ellipse method. It was mainly implemented through ArcGIS 10.5. The specific parameters include centrality, distribution, density, orientation and shape in the standard deviation ellipse method [57]. The overall characteristics of pollutants about temporal dynamic process is analyzed by comparing the changes of these parameters over time.

The elliptic spatial distribution range represents the main area of spatial distribution of geographical elements, the center represents the relative position of its distribution, the azimuth Angle reflects the main trend direction of its distribution, and the long axis represents the degree of dispersion in the main trend direction [58]. The comparison of ellipses with different basic parameters such as size and orientation can provide the difference information of different spatial distributions. Calculation of spatial differentiation coefficient can quantitatively describe the degree of spatial differentiation

among different distributions [58]. The specific formula is as follows:

$$\bar{X} = \sqrt{\frac{\sum_{i=1}^{n}(x_i - \bar{X})^2}{n}}, \bar{Y} = \sqrt{\frac{\sum_{i=1}^{n}(y_i - \bar{Y})^2}{n}},$$

where, $x_i$ and $y_i$ are the spatial coordinate positions of the research elements, $n$ is the total number of the research elements, and $(\bar{X}, \bar{Y})$ is the center of gravity of the ellipse. The direction of the ellipse $\tan\theta$ is based on the $x$ axis, north (12 points direction) as 0 degrees, clockwise rotation, formula is as follows:

$$\tan\theta = \frac{A+B}{C},$$

$$A = \sum_{i=1}^{n} x_i'^2 - \sum_{i=1}^{n} y_i'^2,$$

$$B = \sqrt{\left(\sum_{i=1}^{n} x_i'^2 - \sum_{i=1}^{n} y_i'^2\right)^2 + 4\left(\sum_{i=1}^{n} x_i' y_i'\right)^2},$$

$$C = 2\sum_{i=1}^{n} x_i' y_i',$$

Here, $x_i'$ and $y_i'$ are the coordinate deviation between the research elements $i$ and the mean center. The calculation formula of the axis standard deviation respectively is

$$\sigma_x = \sqrt{\frac{2\sum_{i=1}^{n}(\bar{x}\cos\theta - \bar{y}\sin\theta)^2}{n}},$$

$$\sigma_y = \sqrt{\frac{2\sum_{i=1}^{n}(\bar{x}\sin\theta + \bar{y}\cos\theta)^2}{n}}.$$

The greater of the difference between the long axis and the short axis, the more obvious of the directivity of the research elements; otherwise, the directivity is not obvious.

**2.3.2. Spatial association network feature analysis** Spatial association network feature analysis was to explore the spatial action intensity of PM2.5 and O3 between cities, so as to find the region of pollution source similarity and regional association intensity. The points and lines in the spatial association network constitute the association network of pollutants among

cities. The points represent each city, and the lines represent the spatial association degree of pollutants among cities. The association strength in the network reflects the strength of the relationship between cities [59]. The spatial influence degree of each city is obtained by calculating the spatial association degree of each network node.

**2.3.3. Spatial interpolation** The spatial distribution pattern of PM2.5 and O3 could be studied by spatial interpolation method, to obtain the provincial distribution pattern of PM2.5 and O3 in Liaoning province. Spatial interpolation is a kind of unbiased optimal estimation based on semivariance theory. With the help of ArcGIS10.5, ordinary Kriging interpolation method is adopted to interpolate PM2.5 and O3 mass concentration into continuous data surfaces. Based on uneven distribution of spatial data, the attributes of interpolation points can be comprehensively analyzed [60].

**2.3.4. Exploratory spatial data analysis** The spatial agglomeration and correlation characteristics of PM2.5, O3 and influencing factors in Liaoning province were studied by exploratory spatial data analysis method. Since phenomena in space do not exist in isolation, there is often some correlation, exploratory spatial data analysis can describe the potential interdependence among observation data in the same research area, and provide basis for exploring the spatial-temporal aggregation and evolution of each factor. In order to explore the spatial correlation effect of PM2.5, O3 and each impact factor in Liaoning Province, the multi-factor local Moran model was introduced to explore the spatial agglomeration and correlation characteristics of PM2.5, O3 and each impact factor in Liaoning Province. It conduced based on GeoDa1.2.0. [61]. Its calculation formula is as follows:

$$I_i = \frac{n\dot{(}x_i - \bar{x})}{\sum_{j=1}^{n}(x_j - \bar{x})^2}\sum_{j=1}^{n} w_{ij}(x_j = \bar{x}),$$

where $I_i$ is the local Moran's $I$ statistic, which represents the spatial correlation degree between the region $i$ and its neighboring region. $x_i$ is the observed value of the region $i$. $w_{ij}$ is the spatial weight matrix. The value is 1 if the region $i$ is adjacent to the region $j$, and 0 otherwise. Z test is adopted for the statistical test of local Moran's $I$, that is:

$$Z(I_i) = \frac{I_i - E(I_i)}{\sqrt{var(I_i)}},$$

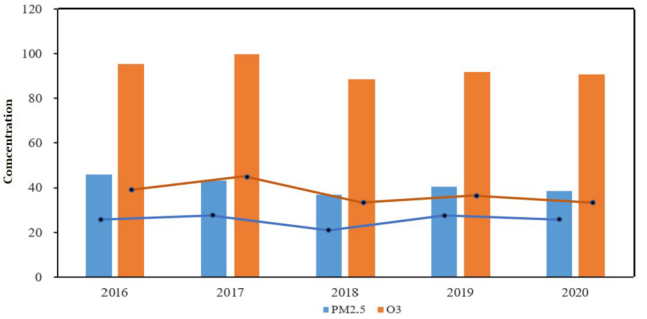


Figure 2: The annual mean values of PM2.5 and O3 in Liaoning province from 2016 to 2020 ($\mu g/m^3$).

When given the significance level of the statistic, $I_i > 0$ and $Z_i > 0$, the region is a high-high agglomeration area; $I_i > 0$ and $Z_i < 0$, the region is a low-low agglomeration area; $I_i < 0$ and $Z_i > 0$, the region is a high-low agglomeration area; $I_i < 0$ and $Z_i < 0$, the region is a low-high agglomeration area.

## 3. Results

### 3.1. Temporal variation characteristics of PM2.5 and O3

The annual mean values of PM2.5 and O3 in 14 cities of Liaoning Province from 2016 to 2020 were calculated (Fig. 2). The annual average concentration of PM2.5 decreased from 45.9 $\mu g/m^3$ in 2016 to 36.7 $\mu g/m^3$ in 2018, with annual decrease rate of 4.6 $\mu g/m^3$. After fluctuation from 2018 to 2020, it decreased to 38.6 $\mu g/m^3$ in 2020. From 2016 to 2018, O3 firstly increased and then decreased. O3 rose again from 2018 to 2020, with large fluctuation range within the year. To sum up, 2018 was an important inflection point for PM2.5 and O3 concentrations in Liaoning Province, reaching the lowest values of 36.7 $\mu g/m^3$ and 88.3 $\mu g/m^3$, respectively. The results showed that PM2.5 mass concentration in all cities decreased gradually, and O3 mass concentration in most cities also decreased slightly. With the decrease of PM2.5 mass concentration, the reduction of O3 contribution rate was not obvious, and O3 pollution could not be ignored. According to the Environmental Air Quality Standard (GB3095-2012), PM2.5 and O3 mass concentrations in 14 cities were close to the moderate level.

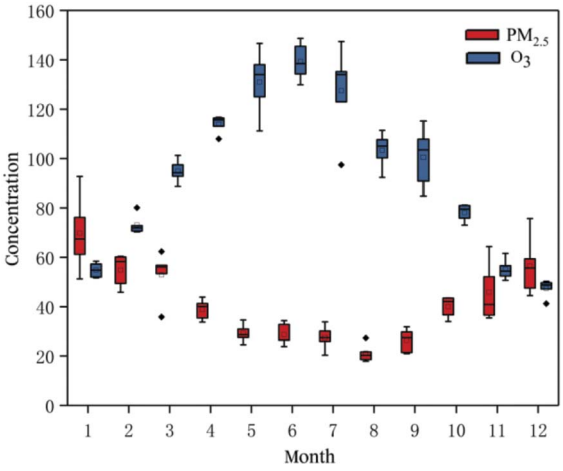


Figure 3: Times series of PM2.5 and O3 in Liaoning province from 2016 to 2020 ($\mu g/m^3$).

The monthly average concentrations of PM2.5 and O3 in Liaoning province from 2016 to 2020 were showed in Fig. 3. PM2.5 and O3 concentrations have obvious seasonal patterns, which were winter > spring > autumn > summer, summer > spring > autumn > winter, respectively. The maximum value of PM2.5 in winter was about 3 times of the minimum value in summer, and the maximum value of O3 in summer was about 3 times of the minimum value in winter. Monthly variation of PM2.5 showed an U-shaped trend, while O3 a significant inverted U-shaped trend (Fig. 3). The monthly O3 average concentrations presented an increasing trend from January to June and August to September, and a decreasing trend from June to August and from September to December, reaching the maximum value in June eventually. On the contrary, the concentration of PM2.5 decreased month by month from January to August, rose month by month from August to December, and reaching its maximum value in January. According to the O3-8h secondary standard ($\geq$ 100 $\mu g/m^3$) and PM2.5 secondary standard ($\geq$ 35 $\mu g/m^3$) in the Environmental Air Quality Standard (GB3095-2012), it could be seen from Fig. 3, the typical period of O3 pollution was from April to September, and the typical period of PM2.5 pollution was from January to March and From October to December.

The temporal dynamic process of PM2.5 and O3 were quantitatively analyzed by standard deviation ellipse method, through ArcGIS spatial statistics module. The parameter results were showed in Table 3 and Table 4, and the visualization results were showed in Fig. 4.

Table 3: The parameters of standard deviation ellipse with PM 2.5

| Item | 2016 | 2017 | 2018 | 2019 | 2020 |
|---|---|---|---|---|---|
| $x$ coordinate of barycenter (km) | 13644971.4 | 13642724.2 | 13639876.9 | 13640191.3 | 13640482.4 |
| $y$ coordinate of barycenter (km) | 5039033.6 | 5036241.1 | 5033869.4 | 5035314.9 | 5033749.7 |
| Standard deviation along the $x$-axis (km) | 202716.5 | 208378.7 | 207785.5 | 207227.6 | 206822.7 |
| Standard deviation along the $y$-axis (km) | 159122 | 157607.9 | 159777.9 | 160786.2 | 160771.9 |
| direction angle (°) | 55.8 | 50.5 | 49.3 | 52.2 | 50.2 |

Table 4: The parameters of standard deviation ellipse with O3

| Item | 2016 | 2017 | 2018 | 2019 | 2020 |
|---|---|---|---|---|---|
| $x$ coordinate of barycenter (km) | 13633071.48 | 13636834.2 | 13636148.4 | 13638078.1 | 13638952.4 |
| $y$ coordinate of barycenter (km) | 5037051.2 | 5035895 | 5031961 | 5032725.4 | 5032935.2 |
| Standard deviation along the $x$-axis (km) | 207267.2 | 203658.7 | 203573.7 | 203957 | 204839.3 |
| Standard deviation along the $y$-axis (km) | 161767.8 | 162017.1 | 163571.6 | 163297.3 | 164225.4 |
| direction angle (°) | 58.3 | 61.7 | 60 | 59 | 59.3 |

The results showed that high concentrations of PM2.5 and O3 were mainly distributed in central and along Bohai Sea of Liaoning province. First of all, there was no significant change with the gravity of PM2.5 and O3 pollutants, which both appeared in northwest Benxi. However, PM2.5 showed a slight trend of southwest shift year by year, while O3 showed a slight trend of southeast shift year by year. The second, the center of standard deviation ellipse of the spatial distribution of PM2.5 and O3 shifted about 5° to the east and 1° to the north, respectively. The overall distribution range of ellipses corresponding to PM2.5 and O3 expanded slightly. The long axis of both of them increased by time. The short axis of PM2.5 increased by time, while the short axis of O3 decreased. The last, the oblateness of the standard deviation ellipse of them gradually increased, which indicated that the direction trend of PM2.5 and O3 was more and more obvious.

### 3.2. The spatial patterns evolution of PM2.5 and O3

As can be seen from Table 5, areas with high level PM2.5 concentrations were found in the central and southwest of Liaoning Province during 2016–2020, including Jinzhou, Anshan, Shenyang and Huludao. While the areas with high concentrations of O3 were located in coastal cities in the middle and west of Liaoning province, i.e., Panjin, Dalian, Huludao, Jinzhou and Yingkou. The areas with low concentration of O3 were mainly distributed in Benxi, Dandong, Liaoyang and Anshan, which were located in the east and part of the central regions in Liaoning. The areas with low concentration of PM2.5 were found in east and south of Liaoning, such as Dalian and Dandong.

In order to deeply explore the spatial action intensity of PM2.5 and O3 among cities in Liaoning Province from 2016 to 2020, the monthly mean data

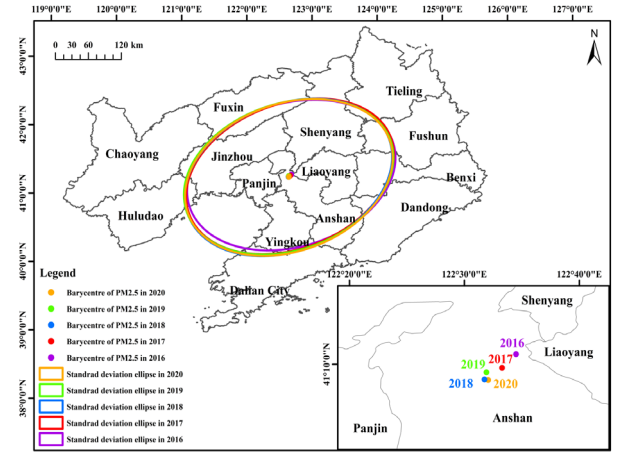


(a)

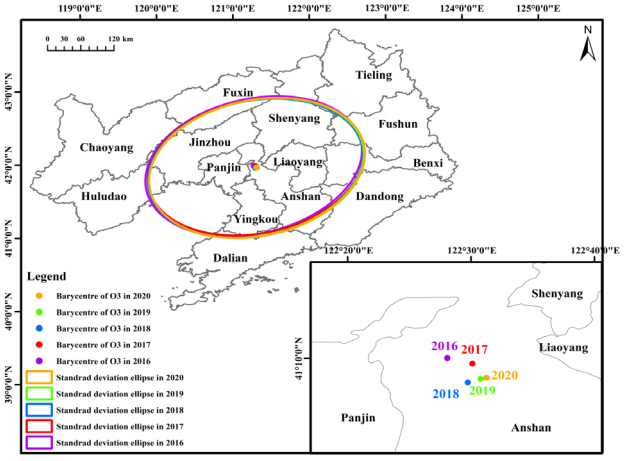


(b)

Figure 4: Spatial distribution pattern and the barycenter of shift path of PM2.5 and O3 in Liaoning province.

of each city were used for spatial association network analysis, and the similarity of pollution sources and regional association intensity were obtained (Fig. 5). For PM2.5, the four urban agglomerations have strong connections, i.e., Chaoyang-Huludao, Panjin-Yingkou-Anshan-Liaoyang-Dandong-Dalian, Fuxin-Shenyang and Tieling-Fushun-Benxi. For O3, Chaoyang-Huludao-Jinzhou-Panjin-Yingkou-Anshan-Liaoyang-Dandong and Fushun-Benxi had relatively consistent for spatial association. Through the analysis of spa-

Table 5: The annual average concentrations of PM 2.5 and O3 in 14 cities (PM 2.5: μg/m$^3$, O3: μg/m$^3$)

| City | PM 2.5 | | | | | O3 | | | | |
|---|---|---|---|---|---|---|---|---|---|---|
| | 2016 | 2017 | 2018 | 2019 | 2020 | 2016 | 2017 | 2018 | 2019 | 2020 |
| Huludao | 46.9 | 46.5 | 40.5 | 46.8 | 42.5 | 105.9 | 104.5 | 92.4 | 92.4 | 92.9 |
| Jinzhou | 55 | 47.3 | 43.8 | 47 | 46.8 | 107.9 | 103.7 | 88.3 | 90.3 | 89.9 |
| Panjing | 39.7 | 39 | 35.2 | 38.9 | 35.6 | 113.3 | 107.3 | 94.8 | 95.6 | 94.3 |
| Yingkou | 44.4 | 42.6 | 39.5 | 42.4 | 40.8 | 114.2 | 112.2 | 103.6 | 101.4 | 96.6 |
| Dandong | 42.2 | 35 | 29 | 32.5 | 29 | 86.2 | 85.8 | 76.4 | 84.7 | 82.7 |
| Dalian | 38.7 | 33.5 | 28.8 | 35.1 | 30 | 106.5 | 105.6 | 93.6 | 97.5 | 95.2 |
| Chaoyang | 39.3 | 40.8 | 35.2 | 37 | 35.6 | 71.9 | 100.7 | 95 | 96.5 | 95 |
| Fuxin | 44 | 38.2 | 32.9 | 37.3 | 36.4 | 83 | 101.1 | 92.4 | 94.5 | 97.8 |
| Shenyang | 53.9 | 49.3 | 39.1 | 42.7 | 41.9 | 94.5 | 99 | 85 | 88.8 | 89.4 |
| Tieling | 48.5 | 48.9 | 38.4 | 41.3 | 39.2 | 96.7 | 97.6 | 81 | 89.3 | 90.9 |
| Liaoyang | 46.9 | 46.8 | 37.7 | 41.5 | 40.8 | 95.1 | 95.5 | 84.2 | 85.2 | 87.1 |
| Anshan | 55.4 | 47.6 | 39.6 | 43.3 | 43.6 | 84.4 | 99.2 | 85.8 | 93.3 | 88.6 |
| Benxi | 44.6 | 40.2 | 32.8 | 36.7 | 34.6 | 82.8 | 77.8 | 75 | 83.4 | 80.8 |
| Fushun | 43.5 | 46.5 | 41.8 | 43.9 | 43 | 96.1 | 91.3 | 88.8 | 93.5 | 92.2 |

tial association network, these urban agglomerations have similar pollution sources or have mutual transmission.

Spatial interpolation has been used to analyze the provincial pattern from January to December in Liaoning province (Fig. 6). The monthly variations of PM2.5 and O3 presented clear trends. That was, the highest PM2.5 concentrations were observed in January, February and December. In January, the concentration of PM2.5 was highest in central Liaoning. The PM2.5 concentration in February was lower than that in January. Beginning in March, PM2.5 concentration showed a declining trend, especially from May to September, PM2.5 concentration in the whole province reached the lowest value of the year. In October, PM2.5 concentrations in central and northern Liaoning began to increase. In November, the increase distribution range of PM2.5 concentration was spread across the province. In December, PM2.5 concentration increased significantly, especially in the central and northern regions. Different from the distribution law of PM2.5 concentration, O3 concentration increased significantly in summer, followed by spring and autumn. The O3 concentration reached the lowest value of the year in November, December, January and February. In March, O3 concentration began to rise. O3 concentration increased significantly in most areas in April. O3 concentration reached the highest value from May to September, and the concentration was the highest in the western and Bohai Sea regions. In October, O3 concentration decreased significantly, only in Bohai Sea region was slightly higher than other areas, and the spatial distribution of low concentration increased gradually.

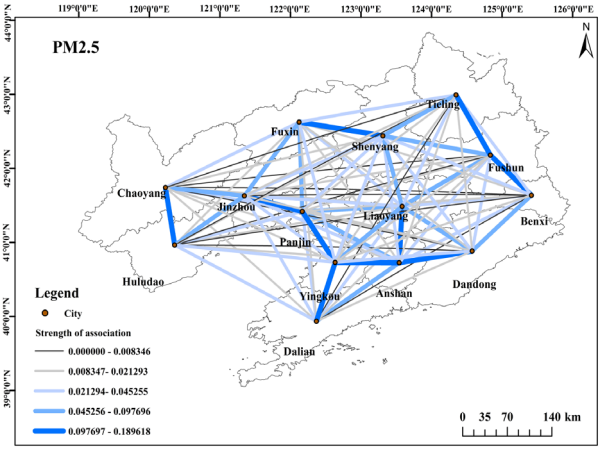


(a)

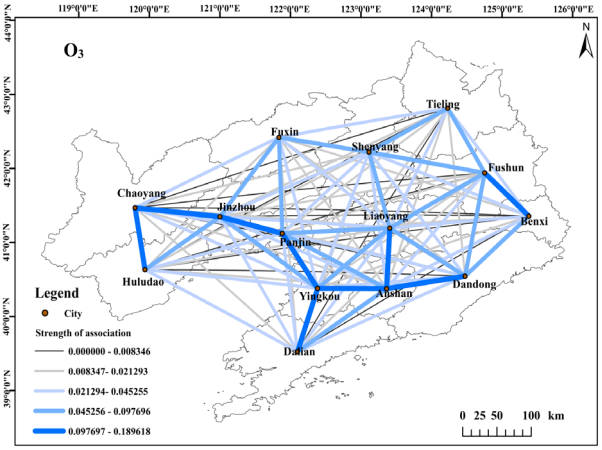


(b)

Figure 5: Spatial association network feature analysis of PM2.5 and O3 in Liaoning province from 2016 to 2020.

### 3.3. The collaborative control of PM2.5 and O3

The ratios of PM2.5 concentration in 2020 to PM2.5 concentration in 2016, and O3 concentration in 2020 to O3 concentration in 2016 were calculated respectively, as showed in Fig. 7. The concentrations of PM2.5 and O3 in Shenyang, Fushun, Benxi, Liaoyang, Tieling, Huludao, Jinzhou, Yingkou, Panjin, Dandong and Dalian showed a downward trend. In Chaoyang, Fuxin

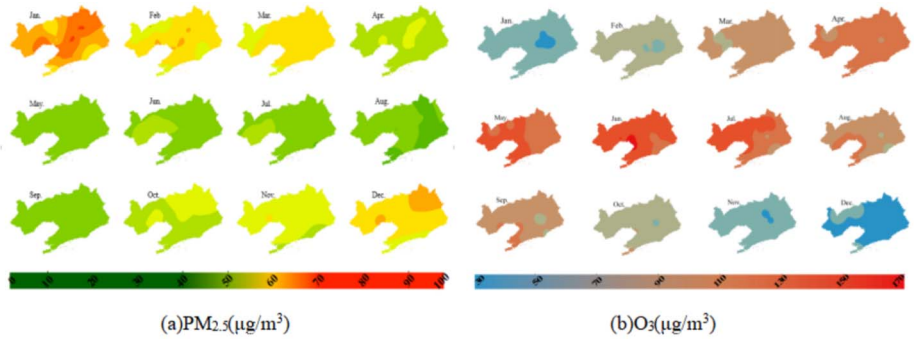


Figure 6: Spatial interpolation diagram of PM2.5 and O3 monthly concentration in Liaoning province.

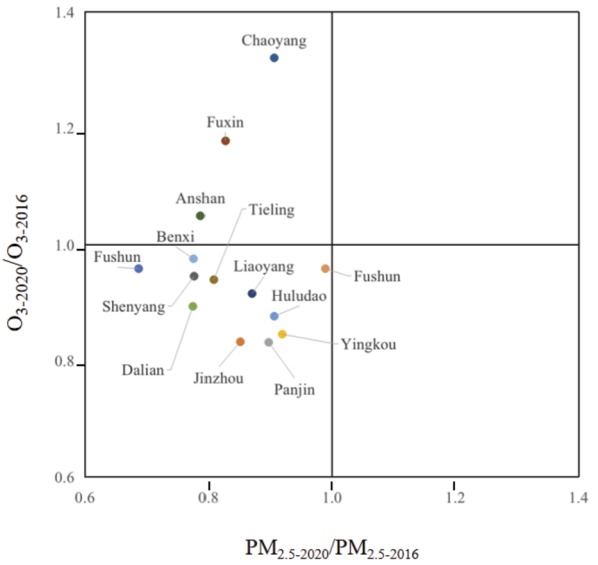


Figure 7: The ratios of PM2.5 and O3 in 14 cities of Liaoning province.

and Anshan, the concentration of PM2.5 presented a downward trend while the concentration of O3 showed an upward trend. It can be seen that from 2016 to 2020, under the influence of a series of policy implementation and human factors, the concentrations of PM2.5 and O3 in all the cities have been improved to some extent. However, it should be pointed out that in Chaoyang, Fuxin and Anshan, it is necessary to strengthen the coordinated control of PM2.5 and O3 to prevent the decline of one pollutant from leading to the rise of another.

Table 6: Moran's analysis of PM2.5 and O3 and economic statistical indicators in Liaoning Province in 2019

| Pointer type | Name of economic indicator | Moran's $I$ |
|---|---|---|
| Agriculture | Primary industry (hundred million yuan) | −0.7137 |
| Agriculture | Fertilizer usage (ten thousand tons) | 0.2108 |
| Industry | Secondary industry (hundred million yuan) | −0.7356 |
| Economics | Gross regional product per capital (yuan/person) | −0.3025 |
| Service Industry | Tertiary industry (hundred million yuan) | −0.9672 |
| Population | Year-end Total (thousands of families) | −0.9771 |
| O3 | The annual mean of O3 | 0.6129 |
| PM2.5 | The annual mean of PM2.5 | 0.1692 |

### 3.4. The influencing factors of PM2.5 and O3

The Moran's index of PM2.5, O3 and the spatial correlation of each impact factor were calculated to deeply analyze the spatial effects of multiple impact factors of PM2.5 and O3. Because of the availability of data, the main economic statistical indicators, PM2.5 and O3 of 14 cities in Liaoning Province in 2019 were only respectively selected. Related economic indicators were agriculture (primary industry and fertilizer usage), industry (secondary industry), gross regional product per capital, service industry (tertiary industry), and population (year-end total). The spatial analysis of multi-factor Moran model was carried out with PM2.5, O3 and major economic statistical indicators (Table 6), all economic indicators passed the significance test ($P \leq 0.05$), and Z test was conducted. The results showed that there were significant differences in the degree of impact in different cities, which needed to be combined with different regions for specific analysis.

Next, the local Moran indices of the concentrations of PM2.5 and O3 and their influencing factors in 14 cities were calculated (Table 7, Table 8) and visualized (Fig. 8). It could be seen that the factors influencing the concentration of PM2.5 and O3 were gross regional product per capital, agriculture, industry, tertiary industry and population density in a descending order.

The high-high agglomeration area of PM2.5 were mainly located in central and northeast areas, including Huludao, Panjin, Shenyang, Tieling, Jinzhou, Benxi and Dandong. The high-high agglomeration area of O3 was mainly concentrated in central and some areas in Bohai Sea regions. The high-high aggregation area of economic factors was in central and western region. The spatial aggregation of primary industry was relatively scattered.

Table 7: Moran's $I$ index of PM2.5 and O3 and economic statistical indexes in 14 cities of 2019

| Name of economic indicator | Huludao | Chaoyang | Jinzhou | Fuxin | Panjin | Shenyang | Tieling |
|---|---|---|---|---|---|---|---|
| Primary industry (hundred million yuan) | −0.17 | −0.11 | −0.04 | −0.98 | 0.28 | −4.06 | 0.00 |
| Fertilizer usage (ten thousand tons) | −0.34 | −0.10 | 1.16 | 1.95 | −0.41 | 0.62 | 0.83 |
| Secondary industry (hundred million yuan) | 0.53 | 0.97 | −0.14 | −0.62 | 0.00 | −5.69 | −1.05 |
| Gross regional product per capital (yuan/person) | 1.09 | 1.97 | −0.28 | 0.19 | −0.58 | −3.95 | −1.00 |
| Tertiary industry (hundred million yuan) | 0.35 | 0.60 | −0.18 | −1.03 | 0.22 | −7.27 | −1.09 |
| Year-end Total (thousands of families) | 0.01 | −0.03 | −0.14 | −1.81 | 0.27 | −7.38 | −0.21 |
| The annual mean of O3 | 0.31 | 1.08 | −0.69 | 0.38 | 0.31 | 1.09 | 0.00 |
| The annual mean of PM2.5 | 1.13 | −1.96 | 1.22 | −0.96 | −1.04 | 1.01 | 0.29 |

Table 8: Moran's $I$ index of PM2.5 and O3 and economic statistical indexes in 14 cities of 2019

| Name of economic indicator | Fushun | Benxi | Liaoyang | Dandong | Anshan | Yingkou | Dalian |
|---|---|---|---|---|---|---|---|
| Primary industry (hundred million yuan) | −0.22 | 0.54 | 0.26 | −0.14 | −1.37 | −0.88 | −3.09 |
| Fertilizer usage (ten thousand tons) | −2.13 | 1.44 | 0.39 | 0.39 | 0.01 | 0.13 | −0.97 |
| Secondary industry (hundred million yuan) | −0.31 | −0.24 | −0.37 | −1.55 | 0.26 | −0.29 | −1.80 |
| Gross regional product per capital (Yuan/person) | −0.03 | −0.01 | −0.07 | −1.56 | 0.04 | 0.98 | −1.05 |
| Tertiary industry (hundred million yuan) | −0.72 | −0.56 | −0.77 | −0.76 | −0.12 | −0.51 | −1.70 |
| Year-end Total (thousands of families) | −0.76 | −1.12 | −1.14 | −0.44 | 0.36 | −0.31 | −0.99 |
| The annual mean of O3 | −1.50 | 5.23 | 4.64 | −0.25 | −0.56 | 0.00 | −1.47 |
| The annual mean of PM2.5 | −0.12 | 0.28 | −0.38 | 2.87 | −0.50 | −0.47 | 0.98 |

The high-high agglomeration area of fertilizer usage was in central and eastern region. High-high agglomeration areas of industrial were in the southwest and Bohai Sea regions. The high-high agglomeration areas of tertiary industry were located in southwest region. The areas with high population density were mainly concentrated in Shenyang, Dalian, Anshan, Tieling and Huludao. These high-high agglomerations indicated that these areas were correspondingly high level agglomerations.

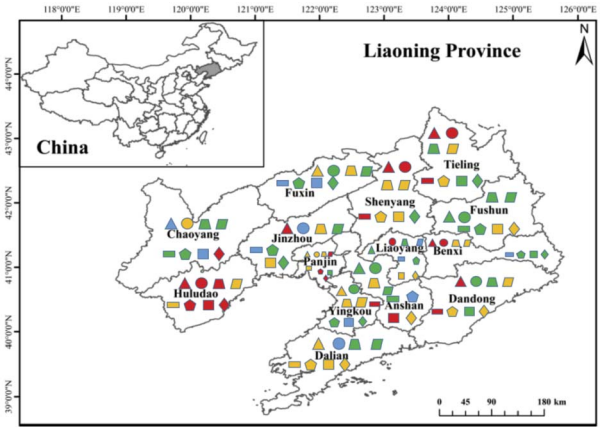


Figure 8: Moran's analysis chart of PM2.5 and O3 and various economic statistical indicators in 14 cities of Liaoning Province in 2019, in which the primary industry is represented by parallelogram, fertilizer usage is represented by rectangle, the secondary industry is represented by isosceles trapezoid, per capital GDP is represented by square, the tertiary industry is represented by diamond shape, population is represented by regular pentagon, PM2.5 is represented by triangle, and O3 is represented by circle. High-high, low-low, high-low and low-high agglomerations areas are showed in red, blue, yellow and green, respectively.

## 4. Discussions

### 4.1. The influencing factors of the temporal variation characteristics of PM2.5 and O3

From 2013 to 2017, with the great efforts to control air pollution in China, air quality improved significantly, as there was a downward trend in PM2.5 and O3 pollutant concentration. After 2018, coordinated emission reduction control measures were taken for PM2.5 and O3 in China, thus pollutant concentrations showed a trend of decline after fluctuation. PM2.5 pollution mostly occurred from October to the following March, and peaked in November and January. This is closely related to the large-scale open-air burning of crop straw and the intensity of coal burning for heating. And during this period, more static and stable weather exacerbated the accumulation of PM2.5 [22]. The change trend of O3 concentration was opposite to that of PM2.5 concentration, with peak values occurring in June and July and

the low values in January and December. Many studies have showed that it was related to the formation mechanism of O3, with high temperature, low humidity and strong light in summer, the emission of volatile organic compounds (VOCs) and nitrogen oxides (NOx) were high and produce photochemical reactions, producing secondary pollutants while generating O3 in the atmosphere [12, 56, 62]. Moreover, Liaoning province is located in high latitude area, with short daylight in winter, which leads to short illumination time and weak illumination, which weaken O3 generation in winter. Therefore, the reverse seasonal distribution characteristics of PM2.5 and O3 concentrations should be paid more attention, and the high incidence of PM2.5 pollution in winter and O3 pollution in summer should be regarded as the key control period. Specifically, it was necessary to improve the combustion efficiency of coal burning, reduce the emission of pollutants from coal burning. Reduced O3 generation by decreasing the emission of volatile organic compounds and nitrogen oxides.

### 4.2. The influencing factors of the spatial patterns evolution of PM2.5 and O3

The high concentration of PM2.5 was mainly found in central and southwestern Liaoning, where industrial production was expanding and densely inhabited district [63]. Studies have showed that the spatial distribution of high O3 concentration was consistent with ground temperature [64]. Moreover, under the influence of high temperature and solar radiation, it was favorable for O3 generation. The temperature of cities in central and western Bohai Sea in Liaoning was higher than that of other cities, so the O3 concentration in this region was higher. It could be seen that spatial distribution of high PM2.5 concentration was different from that of high O3 concentration in some areas. High concentration of O3 enhanced atmospheric oxidation, making gaseous pollutants such as sulfur dioxide and nitrogen oxide in the air more easily oxidized into fine particles such as sulfate and nitrate, thus leading to increase in PM2.5 concentration. High concentration of PM2.5 would weaken solar radiation and reduced O3 photochemical reaction, which was not conducive to O3 generation. There were many factors influencing the correlation between PM2.5 and O3.

### 4.3. Economic factors affecting PM2.5 and O3

Studies have shown that PM2.5 concentration and O3 concentrations in some areas of China is significantly affected by GDP energy consumption,

per capita GDP and population density [65, 66]. PM2.5 and O3 were significantly positively correlated with economic factors in central region, so effectively solving economic factors in central region and increasing investment in ecological environment would play an important role in alleviating local concentrations of PM2.5 and O3 in this region, while economic factors in western China have no significant effect on reducing PM2.5 concentration. PM2.5 and O3 were positively correlated with primary industry in Shenyang, Huludao, Tieling and Panjin, and significantly positively correlated with fertilizer use in central and eastern regions. This suggested that increased agricultural production and fertilizer use would increase the concentration of pollutants in the area. PM2.5 and O3 were positively correlated with industry in Bohai Sea regions. Therefore, industrial emissions from some cities in Bohai Sea regions needed to be considered to mitigate local air pollutant concentrations. For Shenyang, Huludao, Dalian and Tieling, increasing population density would aggravate local air pollution concentration.

## 5. Conclusions

This study analyzed the spatial and temporal distribution characteristics and influencing factors of PM2.5 and O3 in Liaoning Province, which has important reference for environmental management and air pollution control.

First of all, PM2.5 concentration in all cities showed a downward trend in the past five years, and O3 concentration in most cities also decreased slightly. However, with the decrease of PM2.5 concentration, the decrease of O3 concentration was not obvious. PM2.5 concentration was highest in winter, lowest in summer, followed by spring and autumn. In contrast, O3 concentration was highest in summer, followed by spring and autumn, and lowest in winter. The reasons for the opposite seasonal dynamic characteristics were as follows: PM2.5 concentration varied seasonally, which was related to the seasonal characteristics of emission sources. Mainly coal burning for heating, industrial emissions, straw burning, as well as winter inversion and low atmospheric boundary layer. The emission of volatile organic compounded and nitrogen oxide favorable meteorological conditions such as high temperature and strong solar radiation promote O3 generation in summer.

Secondly, PM2.5 concentration was highest in central and southwestern parts of Liaoning province, especially the industrially developed and densely populated areas of Jinzhou, Anshan, Shenyang and Huludao. The high O3 concentration was mainly distributed in the central-western and some cities in Bohai Sea region, including Panjin, Dalian, Huludao, Jinzhou

and Yingkou. The temperature of these cities was higher than that of other cities in the region, which was more conducive to O3 generation. The spatial distribution of PM2.5 and O3 was strongly correlated with population density, environmental factors and meteorological factors. Chaoyang, Fuxin and Anshan should be pay more attention to the coordinated management of PM2.5 and O3.

Finally, the multivariate Moran model showed that PM2.5 and O3 have a certain spatial correlation with economy, agriculture, industry, tertiary industry and population density in a descending order.

## References

[1] J.D. Chen, M. Gao, D. Li, L. Li, M.L. Sun, Q.J. Xie, *Changes in PM2.5 emissions in China: An extended chain and nested refined Laspeyres index decomposition analysis*. Journal of Cleaner Production, **294**:126248, 2021.

[2] A.J. Cohen, M. Brauer, R. Burnett, H.R. Anderson, J. Frostad, K. Estep, K. Balakrishnan, B. Brunekreef, L. Dandona, R. Dandona, V. Feigin, *Estimates and 25-year trends of the global burden of disease attributable to ambient air pollution: An analysis of data from the Global Burden of Diseases Study*. The Lancet, **389**(10082):1907–1918, 2017.

[3] G. Myhre, D. Shindell, Bréon, F.M. Bréon, W. Collins, J. Fuglestvedt, Jin Huang, D. Koch, J.F. Lamarque, D. Lee, B. Mendoza, *Climate Change 2013: The Physical Science Basis. Contribution of Working Group I to the Fifth Assessment Report of the Intergovernmental Panel on Climate Change*. Cambridge University Press, 659–740, 2013.

[4] J. Fuhrer, V.M. Martin, G. Mills, C.L. Heald, H. Harmens, F. Hayes, K. Sharps, J. Bender, *Current and future ozone risks to global terrestrial biodiversity and ecosystem processes*. Ecology And Evolution, **6**(24):8785–8799, 2016.

[5] S.K. Friedlander, *Smoke, Dust and Haze: Fundamentals of Aerosol Behavior*. New York: Wiley Interscience, 1977.

[6] Chinese State Council, *Action plan for the prevention and control of air pollution* (in Chinese), 2013.

[7] MEP, *Three-year action plan to Win the Battle for a Blue Sky* (in Chinese), 2018.

[8] L.L. Qu, S.J. Liu, L.L. Ma, Z.Z. Zhang, Z.Z. Du, J.H. Zhou, Y.H. Meng, *Evaluating the meteorological normalized PM2.5 trend (2014–2019) in the "2 + 26" region of China using an ensemble learning technique*. Environmental Pollution, 115346, 2020.

[9] B. Zhao, H.T. Zheng, S.X. Wang, K.R. Smith, X. Lu, K. Aunan, Y. Gu, *Change in household fuels dominates the decrease in PM2.5 exposure and premature mortality in China in 2005–2015*. Proceedings of the National Academy of Sciences of the United States of America, **115**(49):12401–12406, 2018.

[10] D. Ding, J. Xing, S.X. Wang, K.Y. Liu, J.M. Hao, *Estimated contributions of emissions controls, meteorological factors, population growth, and changes in baseline mortality to reductions in ambient PM2.5 and PM2.5-related mortality in China, 2013–2017*. Environment Health Perspect, **127**(6):067009, 2019.

[11] H.Z. Zheng, L.Y. Xu, *Production and consumption-based primary PM2.5 emissions: Empirical analysis from China's interprovincial trade*. Resources Conservation and Recycling, **155**:104661, 2020.

[12] W. Gao, X.X. Tie, J.M. Huang, R.J. Mao, X.Q. Zhou, G.Q. Chang, *Long-term trend of O3 in a mega City (Shanghai), China: Characteristics, causes, and interactions with precursors*. Science of the Total Environment, **603**:425–433, 2017.

[13] L.B. Gao, T.J. Wang, X.J. Ren, B.L. Zhuang, S. Li, *Sub-seasonal characteristics and meteorological causes of surface O3 in different East Asian summer monsoon periods over the North China Plain during 2014–2019*. Atmospheric Environment, **264**:118704, 2021.

[14] K. Li, D.J. Jacob, H. Liao, L. Shen, Q. Zhang, K.H. Bates, *Anthropogenic drivers of 2013–2017 trends in summer surface ozone in China*. Proceedings of the National Academy of Sciences, **116**(2):422–427, 2019.

[15] D. Ding, J. Xing, S.X. Wang, X. Chang, J. Hao, *Impacts of emissions and meteorological changes on China's ozone pollution in the warm seasons of 2013 and 2017*. Frontiers in Environmental Science, **13**(5):76, 2019.

[16] H.M. Chen, B.L. Zhuang, J. Liu, *Characteristics of ozone and particles in the near-surface atmosphere in the urban area of the Yangtze River Delta, China*. Atmospheric Chemistry And Physics, **19**(7):4153–4175, 2019.

[17] J. Xu, Y.H. Zhang, S.Q. Zheng, Y.J. He, *Aerosol effects on ozone concentrations in Beijing: A model sensitivity study*. Journal Of Environmental Sciences, **24**(4):645–656, 2012.

[18] J. Xing, J.D. Wang, R.R. Mathu, S.X. Wang, *Impacts of aerosol direct effects on tropospheric ozone through changes in atmospheric dynamics and photolysis rates*. Atmospheric Chemistry and Physics, **17**(16):9869–9883, 2017.

[19] Z. Meng, D. Dabdub, J.H. Seinfeld, *Chemical coupling between atmospheric ozone and particulate matter*. Science Citation Index, **277**(5322):116–119, 1997.

[20] Z.Y. Zhang, X.L. Zhang, D.Y. Gong, W.J. Quan, X.J. Zhao, Z.Q. Ma, S.J. Kim, *Evolution of surface O3 and PM2.5 concentrations and their relationships with meteorological conditions over the last decade in Beijing*. Atmospheric Environment, **108**:67–75, 2015.

[21] C.B. Song, L. Wu, Y.C. Xie, J.J. He, *Air pollution in China: Status and spatial-temporal variations*. Environmental Pollution, **227**:334–347, 2017.

[22] X. Lu, J.Y. Hong, L. Zhang, O.R. Cooper, M.G. Schultz, *Severe surface ozone pollution in China: A global perspective*. Environmental Science & Technology, **5**(8):487–494, 2018.

[23] A. Mukherjee, M. Agrawal, *A global perspective of fine particulate matter pollution and its health effects*. Reviews of Environmental Contamination and Toxicology, **244**:5–51, 2017.

[24] Y.H. Wu, W.D. Wang, C. Liu, *The association between long-term fine particulate air pollution and life expectancy in China, 2013 to 2017*. Science of the Total Environment, **712**:136507, 2020.

[25] Q.Y. Guan, F.F. Wang, L.Q. Yang, C.Q. Xu, Z.Y. Liu, *Spatial-temporal variability of particulate matter in the key part of Gansu Province, Western China*. Environmental Pollution, **230**:189–198, 2017.

[26] Z.Y. Liu, Z.L. Qi, X.F. Ni, M.T. Dong, M.Y. Ma, W.B. Xue, Q.Y. Zhang, J.N. Wang, *How to apply* $O_3$ *and* $PM_{2.5}$ *collaborative control to practical management in China: A study based on meta-analysis and machine learning*. Science of the Total Environment, **772**:145392, 2021.

[27] B. Wu, C.Q. Liu, J. Zhang, J. Du, K. Shi, *The multifractal evaluation of* $PM_{2.5}$-$O_3$ *coordinated control capability in China*. Ecological Indicators, **129**:107877, 2021.

[28] J.Y. Zeng, L.Y. Zhang, C.H. Yao, T.T. Xie, L.F. Rao, H. Lu, X.C. Liu, Q.Y. Wang, S.L. Lu, *Relationships between chemical elements of PM2.5 and O3 in Shanghai atmosphere based on the 1-year monitoring observation*. Environmental Science, **95**:49–57, 2020.

[29] P.F. Wang, X. Qiao, H.L. Zhang, *Modeling PM2.5 and O3 with aerosol feedbacks using WRF/Chem over the Sichuan Basin, southwestern China*. Chemosphere, **254**:126735, 2020.

[30] K.W. Li, X.H. Wang, L.M. Li, J. Wang, Y.Y. Liu, *Large variability of O3-precursor relationship during severe ozone polluted period in an industry-driven cluster city (Zibo) of North China Plain*. Journal of Cleaner Production, **316**:128252, 2021.

[31] H.J. Zhao, H.Z. Che, L. Zhang, K. Gui, Y.J. Ma, Y.Q. Wang, H. Wang, Y. Zheng, X.Y. Zhang, *How aerosol transport from the North China plain contributes to air quality in northeast China*. Science of the Total Environment, **738**:139555, 2020.

[32] C.C. Wang, Y.C. Wang, R.F. Ma, J.M. Wang, *Impact of economic agglomeration on pollution of smog based on spatial econometric model: The case study of Yangtze River Delta*. Environmental Research, **28**(1):1–11, 2019.

[33] F.Y. Wang, X.H. Qiu, J.Y. Cao, P. Lin, N.N. Zhang, Y.L. Yan, R.M. Li, *Policy driven changes in the health risk of PM2.5 and O3 exposure in China during 2013–2018*. Science of the Total Environment, **757**:143775, 2021.

[34] Y.P. Luo, M.J. Liu, J. Gan, X.T. Zhou, M. Jiang, R.B. Yang, *Correlation study on PM2.5 and O3 mass concentrations in ambient air by taking urban cluster of Changsha, Zhuzhou and Xiangtan as an example*. Journal of Safety Environment, **15**:313–317, 2015.

[35] Z.S. Wang, D.W. Zhang, Y.T. Li, X. Dong, R.W. Sun, N.D. Sun, *Different air pollution situations of O3 and PM2.5 during summer in Beijing*. Environmental Science, **37**:807–815, 2016.

[36] M.W. Jia, T.L. Zhao, X.H. Cheng, S.L. Gong, X.Z. Zhang, L.L. Tang, D.Y. Liu, X.H. Wu, L.M. Wang, Y.S. Chen, *Inverse relations of PM2.5 and O3 in air compound pollution between cold and hot seasons over an urban area of east China*. Atmospheric, **8**(12):59, 2017.

[37] Y.J. Zhang, T.L. Zhao, C.Z. Ying, Z.F. Wang, B.Z. Ge, D.Y. Liu, X.X. Du, *Seasonal variation of the relationship between surface PM2.5 and*

*O3 concentrations in Xuzhou*. Environmental Science, **39**(6):2267–2272, 2019.

[38] J.J. Chen, H.F. Shen, T.W. Li, X.L. Peng, H.R. Cheng, C.Y. Ma, *Temporal and spatial features of the correlation between PM2.5 and O3 concentrations in China*. International Journal of Environmental Research and Public Health, **16**:4824, 2019.

[39] C. Gong, H. Liao, *A typical weather pattern for ozone pollution events in North China*. Atmospheric Chemistry and Physics, **19**:13725–13740, 2019.

[40] Z.C. Yin, B.F. Cao, H.J. Wang, *Dominant patterns of summer ozone pollution in eastern China and associated atmospheric circulations*. Atmospheric Chemistry and Physics, **19**:13933–13943, 2019.

[41] H.B. Dai, J. Zhu, H. Liao, J.D. Li, M.X. Liang, Y. Yang, X. Yue, *Co-occurrence of ozone and PM2.5 pollution in the Yangtze River Delta over 2013–2019: Spatial-temporal distribution and meteorological conditions*. Atmospheric Research, **249**:105363, 2020.

[42] Boreddy, K.R. Suresh, Mochizuki, Tomoki, Kawamura, Kimitaka, Bikkina, Srinivas, M.M. Sarin, *Homologous series of low molecular weight (C1–C10) monocarboxylic acids, benzoic acid and hydroxyacids in fine-mode (PM2.5) aerosols over the Bay of Bengal: Influence of heterogeneity in air masses and formation pathways*. Atmospheric Environment, **167**:170–180, 2017.

[43] H.G. Tao, J. Xing, H.S. Zhou, J. Pleim, L.M. Ran, X. Chang, S.X. Wang, F. Chen, H.T. Zheng, J.H. Li, *Impacts of improved modeling resolution on the simulation of meteorology, air quality and human exposure to PM2.5, O3 in Beijing, China*. Journal of Cleaner Production, **243**:118574, 2020.

[44] S. Zhang, D.P. Li, S.S. Ge, S.J. Liu, C. Wu, Y.Q. Chen, *Rapid sulfate formation from synergetic oxidation of SO2 by O3 and NO2 under ammonia-rich conditions: Implications for the explosive growth of atmospheric PM2.5 during haze events in China*. Science of the Total Environment, **772**:144897, 2021.

[45] W.J. Duan, X.Q. Wang, S.Y. Cheng, R.P. Wang, J.X. Zhu, *Influencing factors of PM2.5 and O3 from 2016 to 2020 based on DLNM and WRF-CMAQ*. Environmental Pollution, **285**:117512, 2021.

[46] Z. Yang, J. Yang, M.M. Li, J.J. Chen, C.Q. Ou, *Nonlinear and lagged meteorological effects on daily levels of ambient PM2.5 and O3:*

*Evidence from 284 Chinese cities*. Journal Of Cleaner Production, **278**:123931, 2021.

[47] Y.Y. Zeng, Y.F. Cao, X. Qiao, B.C. Seyler, Y. Tang, *Air pollution reduction in China: Recent success but great challenge for the future*. Science of the Total Environment, **663**:329–337, 2019.

[48] J. Zhang, L. Liu, Y.Y. Wang, Y. Ren, X. Wang, Z.B. Shi, D.Z. Zhang, H.Z. Che, H.J. Zhao, Y.F. Liu, *Chemical composition, source, and process of urban aerosols during winter haze formation in Northeast China*. Environmental Pollution, **231**:357–366, 2017.

[49] Y.C. Li, J. Liu, H. Han, T.L. Zhao, X. Zhang, B.L. Zhuang, T.J. Wang, H.M. Chen, Y. Wu, M.M. Li, *Collective impacts of biomass burning and synoptic weather on surface PM2.5 and CO in Northeast China*. Atmospheric Environment, **213**:64–80, 2019.

[50] F. Cao, S.C. Zhang, K. Kawamura, Y.L. Zhang, *Inorganic markers, carbonaceous components and stable carbon isotope from biomass burning aerosols in Northeast China*. Science of the Total Environment, **572**:1244–1251, 2016.

[51] F. Cao, S.C. Zhang, K. Kawamura, X.Y. Liu, C. Yang, Z.F. Xu, M.Y. Fan, W.Q. Zhang, M.Y. Bao, Y.H. Chang, *Chemical characteristics of dicarboxylic acids and related organic compounds in PM2.5 during biomass-burning and non-biomass-burning seasons at a rural site of Northeast China*. Environmental Pollution, **231**:654–662, 2017.

[52] W.W. Chen, Y. Liu, X.W. Wu, Q.Y. Bao, Z.T. Gao, X.L. Zhang, H.M. Zhao, S.C. Zhang, A.J. Xiu, T.H. Cheng, *Spatial and temporal characteristics of air quality and cause analysis of heavy pollution in northeast China*. Environmental Science, **40**:4810–4823, 2019.

[53] L.L. Li, K. Wang, W.W. Chen, Q.L. Zhao, L.J. Liu, W. Liu, Y. Liu, J.Q. Liu, J.M. Zhang, *Atmospheric pollution of agriculture-oriented cities in Northeast China: A case in Suihua*. Journal Of Environmental Sciences, **97**:85–95, 2020.

[54] J. Zhang, L. Liu, L. Xu, Q.H. Lin, H.J. Zhao, Z.B. Wang, S. Guo, M. Hu, D.T. Liu, Z.B. Shi, D. Huang, W.J. Li, *Exploring wintertime regional haze in Northeast China: Role of coal and biomass burning*. Atmospheric Chemistry and Physics, **20**:5355–5372, 2020.

[55] L.L. Li, K. Wang, Z.J. Sun, W.Y. Wang, H. Qi, *Bottom-up emission inventory and its spatio-temporal distribution from paved road dust based*

*on field investigation: A case study of Harbin, Northeast China*. Atmospheric, **12**:449, 2021.

[56] L. Anselin, *The future of spatial analysis in the social sciences*. Science Citation Index, **5**(2):67–76, 1999.

[57] T. Zhou, A.Y. Niu, J.J. Ma, S.J. Xu, *Spatial-temporal pattern of national wetland parks*. Journal of Natural Resources, **34**(1):26–39, 2019.

[58] L. Zhao, Z.Q. Zhao, *Projecting the spatial variation of economic based on the specific Ellipses in China*. Scientia Geographica Sinica, **34**(8):979–986, 2014.

[59] Y. Feng, M.Y. Hou, S.B. Yao, *Structural characteristics and formation mechanism of spatial Correlation network of grain production in China*. Scientia Geographica Sinica, **75**(11):2380–2395, 2020.

[60] X.M. Huang, J.B. Zhao, J.J. Cao, Y. Song, *Temporal and spatial variation characteristics and driving factors of O3 concentration in Chinese cities*. Environmental Science, **40**(3):1120–1131, 2019.

[61] N. Wang, X.P. Lu, X.J. Deng, X. Huang, F. Jiang, A.J. Ding, *Aggravating O3 pollution due to NOx emission control in eastern China*. Science of the Total Environment, **677**:732–744, 2019.

[62] L. Wang, W.J. Wang, Z.F. Wu, H.B. Du, X.J. Shen, S. Ma, *Spatial and temporal variations of summer hot days and heat waves and their relationships with large-scale atmospheric circulations across Northeast China*. International Journal Of Climatology, **38**:5633–5645, 2018.

[63] H.J. Zhao, K. Gui, Y.J. Ma, Y.F. Wang, Y.Q. Wang, H. Wang, Y. Zheng, L. Li, L. Zhang, H.Z. Che, X.Y. Zhang, *Climatology and trends of aerosol optical depth with different particle size and shape in northeast China from 2001 to 2018*. Science of the Total Environment, **763**:142979, 2021.

[64] Y.Y. Wang, H.Y. Du, Y.Q. Xu, D.B. Lu, X.Y. Wang, Z.Y. Guo, *Temporal and spatial variation relationship and influence factors on surface urban heat island and ozone pollution in the Yangtze River Delta, China*. Science of the Total Environment, **631–632**:921–933, 2018.

[65] Y.R. Yao, C. He, S.Y. Li, W.C. Ma, S. Li, Q. Yu, N. Mi, J. Yu, W. Wang, L. Yin, Y. Zhang, *Properties of particulate matter and gaseous pollutants in Shandong, China: Daily fluctuation, influencing factors, and spatio-temporal distribution*. Science of the Total Environment, **660**:384–394, 2019.

[66] M.Z. Du, W.J. Liu, Y.Z. Hao, *Spatial correlation of air pollution and its causes in Northeast China*. International Journal of Environmental Research and Public Health, **18**:10619, 2021.

Hongmei Yang
Institute for Mathematical Sciences
Renmin University of China
Beijing 100872
China
School of Mathematics and Data Sciences
Changji University
Xinjiang 831100
China
*E-mail address:* 20813524@qq.com

Yanqi Liu
Key Laboratory of Land Surface Pattern and Simulation
Institute of Geographic Sciences and Natural Resources Research
Chinese Academy of Sciences
Beijing 100101
China
*E-mail address:* 2438015461@qq.com

Xiaoqiu Jiang
International Poverty Reduction Center in China
Beijing 100028
China
*E-mail address:* jiangxiaoqun@iprcc.org.cn

Xinqi Gong
Institute for Mathematical Sciences
Renmin University of China
Beijing 100872
China
*E-mail address:* xinqigong@ruc.edu.cn

Received January 28, 2023